Proceedings of the Estonian Academy of Sciences,
2013, **62**, 2, 133–140
doi: 10.3176/proc.2013.2.07
Available online at www.eap.ee/proceedings

COMPUTATIONAL CHEMISTRY

Computational study of the copper-free Sonogashira cross-coupling reaction: shortcuts in the mechanism

Lauri Sikk*, Jaana Tammiku-Taul, and Peeter Burk

Institute of Chemistry, University of Tartu, Ravila 14A, 50411 Tartu, Estonia

Received 14 May 2012, accepted 31 July 2012, available online 7 May 2013

Abstract. The *sec*-butylammonium salt catalysed oxidative addition of phenyl bromide to tris(triphenylphosphane)palladium and reaction of phenylacetylene with *cis*-$Pd(PPh_3)_2(Ph)Br$ were modelled using DFT B97D/cc-pVDZ method to study the mechanism of the copper-free Sonogashira cross-coupling reaction. *sec*-Butylammonium bromide influences the oxidative addition by coordinating with palladium catalyst and the resulting product is *trans*-$Pd(PPh_3)_2(Ph)Br$, not the corresponding *cis*-compound, which is formed in the absence of salt. The transition-state energy of this oxidative addition mechanism is very close to the previously reported biligated oxidative addition pathway. Reaction of acetylene with *cis*-$Pd(PPh_3)_2(Ph)Br$ can lead to either a *trans*- or a *cis*-$Pd(PPh_3)_2(CCPh)Ph$ complex, while only the latter is capable of undergoing reductive elimination.

Key words: Sonogashira, cross-coupling, density functional theory, palladium, copper-free.

INTRODUCTION

The Sonogashira cross-coupling reaction takes place between aryl halide (ArX) and terminal acetylene, catalysed by a zerovalent palladium catalyst to produce diyne (see Fig. 1).

It belongs to the family of palladium-catalysed cross-coupling reactions, which have been a valuable tool for organic synthesis since their discovery [1–3]. In a typical Sonogashira cross-coupling reaction, copper is used as a co-catalyst, but a series of copper-free Sonogashira reactions have been developed to suppress homocoupling of the terminal acetylenes [4,5]. The mechanism of the catalytic cycle has not been extensively studied, although some computational papers on the full catalytic cycle have been published [6–11]. The reaction mechanism is similar to other palladium-catalysed cross-coupling reactions and it consists of oxidative addition, *cis–trans* isomerization, deprotonation (also called alkynylation), and reductive eliminantion steps. Oxidative addition (reaction of aryl halide with a zerovalent palladium catalyst) is often described as a rate-limiting step, and numerous papers are dedicated to the experimental and theoretical investigations of its kinetics and mechanism [12–15]. Many authors have demonstrated that halide anions in the reaction mixture accelerate the oxidative addition [16–19], but our recent computational study in dichloromethane solution revealed that halide anions alone are not responsible for the increase of the reaction rate [9]. These results are backed up by the experimental work of Barrios-Landeros et al., who showed that both the halide ion and the corresponding cation of organic base play an important role in the reaction [20]. The product of oxidative addition, *cis*-PdL_2ArX, can isomerize to the corresponding *trans*-complex. This reaction is usually fast and many reaction mechanisms are possible [21,22].

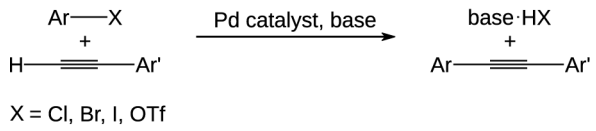

Fig. 1. Copper-free Sonogashira cross-coupling reaction.

* Corresponding author, Lsikk@ut.ee

The deprotonation step in the Sonogashira cross-coupling is a reaction between terminal acetylene and the product of oxidative addition and results in $PdL_2Ar(C{\equiv}CAr')$. The deprotonation step, starting from the *trans*-PdL_2ArX complex, is usually accepted as the dominant reaction pathway [4,23–25], but at the same time a similar reaction can take place with the corresponding *cis*-isomer, which is especially important for chelating ligands, where the formation of *trans*-PdL_2ArX is not possible [15]. The last step of the catalytic cycle is reductive elimination, where a new carbon–carbon bond is formed and the catalyst is regenerated. Aside from the traditional mechanism described in this paper, an alternative carbopalladation pathway was described by Ljungdahl and coworkers [26].

The aim of the current study was to model computationally some "non-classical" and less-studied pathways in the copper-free Sonogashira cross-coupling reaction. First, the oxidative addition step, co-catalysed by *sec*-butylammonium bromide, was studied to test the reaction pathway proposed by Barrios-Landeros et al. [20]. Secondly, we studied two different mechanisms of the deprotonation step starting from *cis*-PdL_2ArX to elucidate their feasibility relative to the earlier studied isomerization of *cis*-PdL_2ArX to *trans*-PdL_2ArX and the following deprotonation [9].

THEORETICAL MODEL

The study of the copper-free Sonogashira cross-coupling reaction was carried out by determining the structures corresponding to ground states and transition states on the reaction energy hypersurfaces.

The copper-free Sonogashira coupling between phenyl bromide (PhBr) and phenylacetylene (PhC≡CH) was modelled, where tetrakis(triphenylphosphano)palladium ($Pd(PPh_3)_4$) was used as a catalyst and *sec*-butylamine (*sec*-$BuNH_2$) as a base. Being small enough for computational study, these reagents are used in the synthesis of disubstituted acetylenes. As *sec*-$BuNH_2$ has two enantiomers commonly used as a racemic mixture, we performed the calculations using *S*-*sec*-$BuNH_2$ in order to minimize the computational cost.

All calculations were performed with Gaussian 09 program package [27] using density functional theory (DFT) with hybrid B97D functional [28,29] and the cc-pVDZ basis set [30]. In the case of palladium, Stuttgart–Dresden effective core potentials with accompanying basis sets were used (obtained from EMSL Basis Set Exchange) [31,32]. Harmonic frequency analysis was used to confirm correspondence of the found structures either to minima (number of imaginary frequencies equals zero) or transition states (number of imaginary frequencies equals one). Unscaled frequencies from vibrational analysis were also used to get enthalpies and free energies in the standard state (1 atm and 298.15 K). In the following discussion enthalpies are used to characterize the energies of stationary points found on the potential energy surface (PES), as computational methods are less accurate for predicting entropies and free energies than enthalpies [33]. Intrinsic reaction coordinate (IRC) analysis was used to verify that the obtained transition state connects reactants and products [34,35]. All geometry optimizations and frequency calculations were performed in dichloromethane (DCM) using the continuum solvation model SMD [36]. Dichloromethane was chosen as a solvent, as it is widely used in both NMR measurements and synthetic procedures. More importantly, DCM is a weakly coordinating solvent, thus, non-inclusion of specific solvent effects is justified. The free energy values were corrected to 1 mol/L standard state [37].

RESULTS AND DISCUSSION

Oxidative addition

In our previous paper, we reported four different oxidative addition pathways (monoligated, biligated, anion-assisted, and base-assisted mechanisms), among which the biligated pathway had the lowest-energy transition state (ΔH = 29.1 kcal/mol, ΔG = 28.2 kcal/mol, relative to the starting compounds) [9]. The anion-assisted oxidative addition pathway is much higher in energy (mainly due to the separation of charges in apolar solvent), and a further investigation of the halide ion influence on the oxidative addition was required. The mechanism proposed here is based on the experimental work by Barrios-Landeros et al. [20].

As noted in our previous paper, the active palladium catalyst is $Pd(PPh_3)_3$ (**1**, Scheme 1), which undergoes the oxidative addition through a series of association and dissociation steps [9].

The first step is the coordination of *sec*-butylammonium bromide (which is a product of the Sonogashira cross-coupling reaction) to palladium complex **1**. This reaction is exothermic (ΔH = –9.5 kcal/mol, ΔG = 1.3 kcal/mol), and the Br–Pd distance in the resulting complex **2** is 4.592 Å. The subsequent ligand dissociation and the formation of trigonal planar complex **3** decreases the Br–Pd bond length to 2.893 Å, which is mainly due to the steric effects of the ligands. The bromine atom lies slightly above the P–Pd–P plane (by 14.4°) and the P–Pd–P angle is 132.9°. The subsequent ligand dissociation gives rise to complex **4**, where the phosphane ligand and Br are in the *trans* position (P–Pd–Br angle is 170.5°) and one hydrogen atom of the amino group of *sec*-butylammonium ion interacts with palladium (Pd–H distance is 2.817 Å), while the other hydrogen atom is

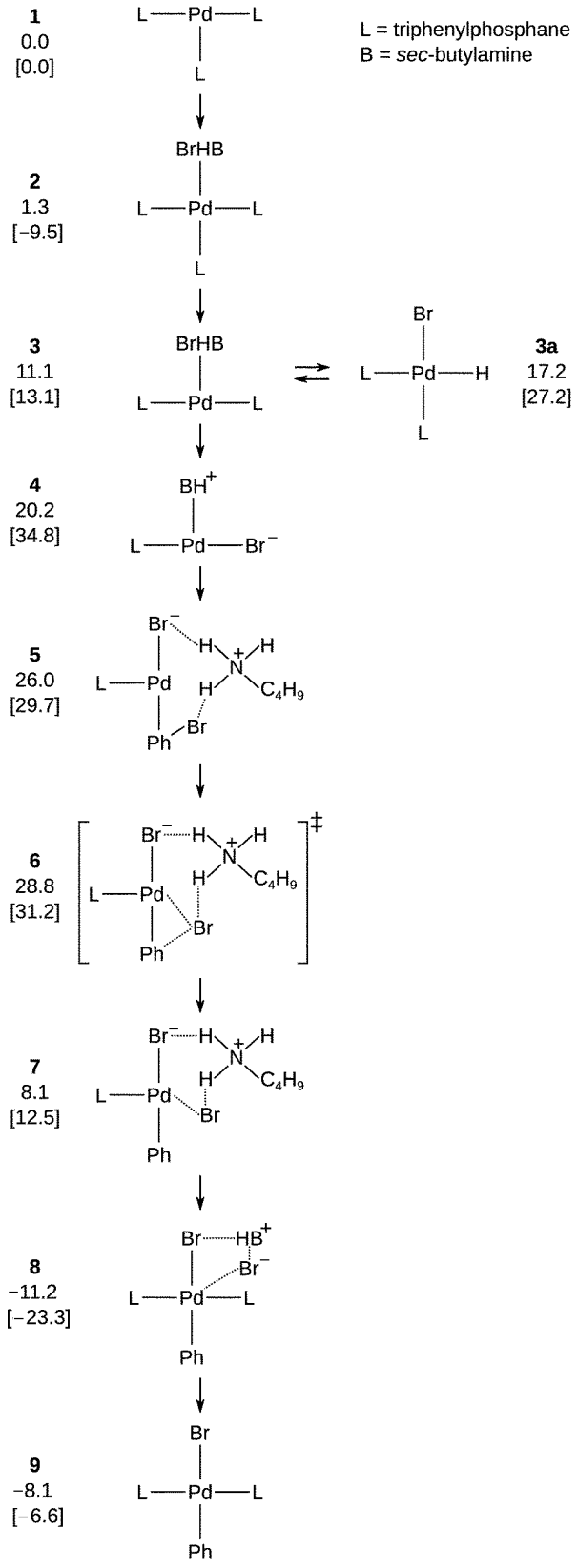

Scheme 1. Salt-assisted mechanism of oxidative addition. Free energies and enthalpies (in square brackets) are in kcal/mol, relative to starting compounds.

directed toward bromine atom (Br–H distance is 2.336 Å). Coordination of phenyl bromide to **4** results in complex **5**, where bromine atom, originating from ammonium salt, is located in the *trans* position relative to phenyl bromide, and *sec*-butylammonium cation is acting as a bridge between the two bromine atoms. Palladium atom interacts with carbons 1 and 2 of phenyl bromide (Pd–C distances are 2.126 Å and 2.241 Å, respectively). This interaction increases the Br–C bond distance in phenyl bromide (2.056 Å in complex **5**, 1.935 Å in free phenyl bromide). The geometry of complex **4** was confirmed by the removal of phenyl bromide from complex **5** and the subsequent geometry optimization. Structure **5** is followed by transition state **6**, which is by 28.8 kcal/mol higher in free energy and by 31.2 kcal/mol higher in enthalpy than the starting compounds. The imaginary frequency of the transition state **6** corresponds to the increase in the C–Br bond length, while the Pd–C bond length is 2.014 Å. Transition state **6** is followed by complex **7**, which can be described as a *trans*-PdL(Ph)Br complex with *sec*-butylammonium bromide. In this complex, the phenyl group and bromine atom are in the *trans* position, while the bromide ion of the ammonium salt is above the C–Pd–P plane (Pd–Br distance is 4.360 Å), and the *sec*-butylammonium cation acts as a bridge between the two bromine atoms. The subsequent addition of phosphane ligand results in a *trans*-PdL_2(Ph)Br complex with *sec*-butylammonium bromide (**8**), which gives the end product of oxidative addition (*trans*-PdL_2(Ph)Br, **9**) after the dissociation of the ammonium salt. One could argue that the dissociation of the ammonium salt from complex **7** would also be a viable pathway, but as we were unable to find a minimum for the *trans*-PdL(Ph)Br complex (all geometry optimizations resulted in the *cis*-PdL(Ph)Br complex), this reaction route was ruled out.

Complex **3** can form *cis*-PdL_2(H)(Br) (**3a**) through the loss of *sec*-butylamine. Barrios-Landeros et al. showed that in the case of P^tBu_3 ligands, complex **3a** is more reactive toward phenyl bromide than $Pd(P^tBu_3)_2$ [20]. Contrary to that, we were unable to find oxidative-addition pathways involving complex **3a**. The transition state energies of the previously reported biligated oxidative addition pathway [9] and the salt-catalysed pathway described here are very close (enthalpies 29.1 and 31.2 kcal/mol; free energies 28.2 and 28.8 kcal/mol, respectively, relative to starting compounds). The difference is so small that on the basis of these calculations it is very hard to correctly evaluate which of these pathways is energetically favoured.

It is important to note that in the product of oxidative addition (complex **9**) bromine atom and phenyl group are in the *trans* position. This suggests that after a few catalytic cycles, when enough ammonium salt is produced in the reaction (see Fig. 1), the copper-free Sonogashira cross-coupling can switch

to the salt-catalysed oxidative addition pathway and, thus, omit the *cis–trans* isomerization step.

Deprotonation

The product of oxidative addition reacts with alkyne in the presence of base resulting in the $PdL_2(PhCC)Ph$ complex. The base is required to deprotonate the alkyne and is sometimes used as a solvent in the copper-free Sonogashira reactions [5]. The isomerization of the oxidative addition product *cis*-$Pd(PPh_3)_2(Ph)Br$ to *trans*-$Pd(PPh_3)_2(Ph)Br$ is usually very fast [38] and therefore, the *trans*-complex is generally accepted as the starting point of the deprotonation step. On the other hand, bidentate ligands, which cannot form this type of *trans*-complexes, have been successfully used in the copper-free Sonogashira reaction [39] and the reaction of *cis*-$Pd(PPh_3)_2(Ph)Br$ with alkyne should be considered as a possible reaction pathway. In the next section of this article, we report the computationally obtained reaction mechanisms for deprotonation that starts from the *cis*-$Pd(PPh_3)_2(Ph)Br$ complex. These are alternative routes to the mechanism of deprotonation reaction described in our previous article [9].

The formation of *cis*-$Pd(PPh_3)_2(Ph)Br$ (Sheme 2, **10**) from $Pd(PPh_3)_3$ and phenyl bromide is exothermic ($\Delta H = -5.0$ kcal/mol, $\Delta G = -4.0$ kcal/mol) and leads to two deprotonation pathways.

The first deprotonation mechanism of the *cis*-$Pd(PPh_3)_2(Ph)Br$ complex (Scheme 2, I) starts with the dissociation of the phosphane ligand in the *trans* position to the phenyl group and the formation of the *cis*-$Pd(PPh_3)(Ph)Br$ complex (Scheme 2, **11**). The consecutive coordination of phenylacetylene and *sec*-butylamine to **11** are both exothermic and give rise to complexes **12** and **13**, respectively, where the triple bond of phenylacetylene is perpendicular to the Br–Pd–P plane. The imaginary frequency of the transition state of the *trans*-deprotonation step (**14**) corresponds to the elongation of the C–H bond of the acetylenic proton. This transition state leads to structure (**15**), which, in turn, forms the anionic *trans*-$Pd(PPh_3)(CCPh)PhBr^-$ complex (**16**) after the dissociation of the protonated base. Due to the formation of charged species, this reaction is endothermic ($\Delta\Delta H =$ 23.1 kcal/mol and $\Delta\Delta G = 11.9$ kcal/mol). Complex **16** can release bromide ion to generate *sec*-butylammonium bromide and the monoligated species **17**, which can form the biligated complex **18** as the end product of *trans*-deprotonation pathway. This deprotonation mechanism leads to the palladium complex where the phenyl- and phenylacetylenic groups are in the *trans* position. A previous mechanistic study showed that this type of complex is unable to undergo reductive elimina-

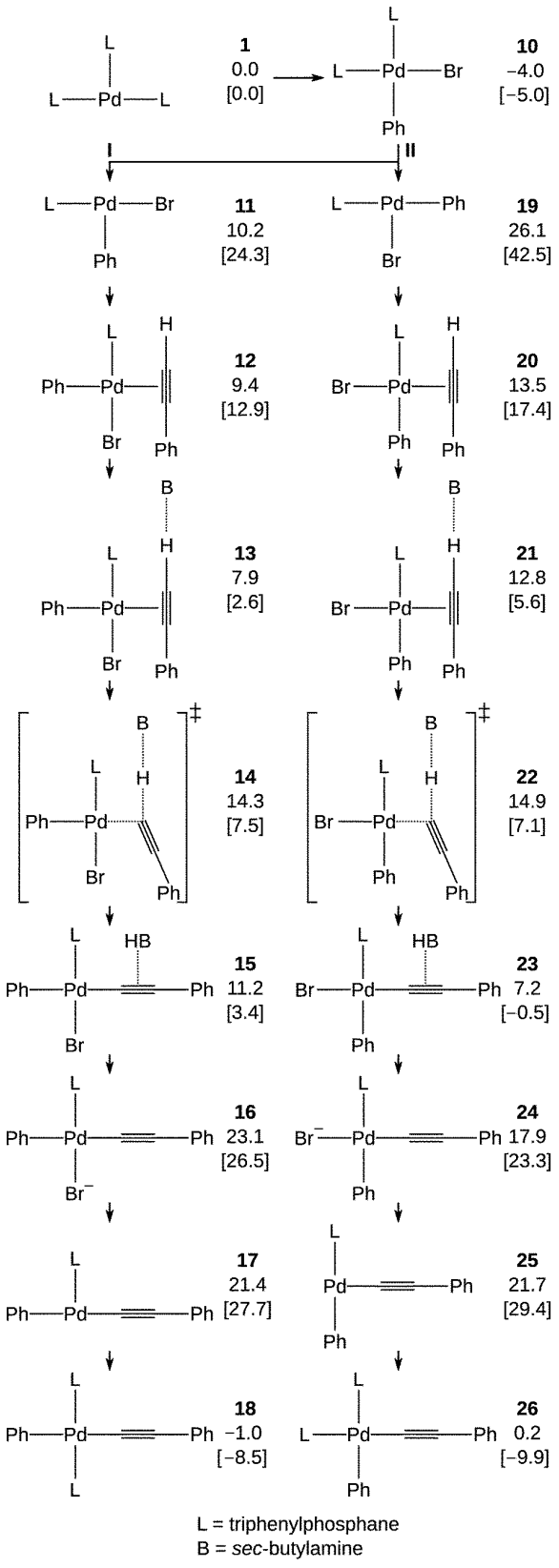

Scheme 2. Mechanisms of *trans*-(I) and *cis*-(II) deprotonation. Free energies and enthalpies (in square brackets) are in kcal/mol, relative to the starting compounds.

tion and the isomerization to the corresponding *cis*-complex is very slow [40]. On the basis of these results we can treat this deprotonation mechanism as "unproductive" in the overall reaction scheme, leading to a reduced concentration of the active palladium catalyst.

The *cis*-deprotonation mechanism of the *cis*-$Pd(PPh_3)_2(Ph)Br$ complex (Scheme 2, II) starts with the dissociation of the triphenylphosphane ligand in the *cis* position to the phenyl group from complex **10** and the formation of the *cis*-$Pd(PPh_3)(Ph)Br$ complex (Scheme 2, **19**). We can see that the ligand dissociation from the *trans* position to the phenyl group is energetically favoured ($\Delta\Delta H$ = 29.3 kcal/mol and $\Delta\Delta H$ = 47.5 kcal/mol, respectively) compared to the dissociation from the *cis* position (Scheme 2, **11**). This large difference in the reaction enthalpies can be attributed to the larger *trans*-effect of the phenyl group compared to bromine atom. The *cis*-deprotonation mechanism proceeds similarly to the previously described *trans*-deprotonation mechanism: the consecutive addition of phenylacetylene and base results in the formation of complexes **20** and **21**. Similarly to **14**, the imaginary frequency of transition state **22** corresponds to the elongation of the C–H bond of the acetylenic proton. Transition state **22** leads to the formation of the *cis*-$Pd(PPh_3)(CCPh)PhBr^-$ complex (**23**). The dissociation of the *sec*-butylammonium cation from complex **23** leads to *cis*-$Pd(PPh_3)(CCPh)PhBr^-$ (**24**), where the phenyl- and phenylacetylenic groups are in the *cis* position. Similarly to **16**, the bromine atom can be substituted by triphenylphosphane ligand to generate *cis*-$Pd(PPh_3)_2(CCPh)Ph$ (**26**) through the monoligated intermediate **25**. The end product of the *cis*-deprotonation mechanism (**26**) is the starting point for the lowest-energy reductive elimination pathway leading to the formation of diphenylacetylene and the regeneration of the catalyst [9].

The deprotonation mechanism starting with the substitution of bromine atom in the *cis*-$Pd(PPh_3)_2(Ph)Br$ complex (**10**) to phenylacetylene was also investigated. However, the transition state corresponding to the deprotonation of alkyne in this complex was not found.

Comparing these two deprotonation pathways of the *cis*-$Pd(PPh_3)_2(Ph)Br$ complex, the *cis*- and *trans*-deprotonation mechanisms may seem to occur at the same rate as the energies of transition states **14** and **22** are very close. On the other hand, the first intermediate in the *cis*-deprotonation pathway (**19**) has much higher energy than the transition states, indicating that the *trans*-deprotonation mechanism is favoured over the *cis*-deprotonation mechanism. It should be kept in mind that the *trans*-deprotonation pathway leads to the formation of *trans*-$Pd(PPh_3)_2(CCPh)Ph$ (**18**), which cannot undergo reductive elimination. Moreover, the product of transition state **14** is higher in energy than the reactants, indicating that the *trans*-deprotonation pathway is shifted toward the formation of reactants.

The computational modelling of these two deprotonation pathways suggests that although a reaction between phenylacetylene and *cis*-$Pd(PPh_3)(Ph)Br$ is possible, the previously reported isomerization to *trans*-$Pd(PPh_3)(Ph)Br$ and the subsequent reaction with phenylacetylene are energetically favoured [9]. However, the studied mechanisms may be important in the case of chelating ligands, where the formation of a *trans*-complex is impossible.

Complete catalytic cycle

By combining the computational results described here with our previous findings [9], a general mechanism for the copper-free Sonogashira cross-coupling reaction can be constructed. The full catalytic cycle starts with the oxidative addition of aryl halide to the palladium catalyst $Pd(PPh_3)_3$, which can result in either a *cis*- or a *trans*-complex (Scheme 3, routes A and A′, respectively). The isomerization of *cis*-$Pd(PPh_3)_2(Ph)Br$ to the corresponding *trans*-$Pd(PPh_3)_2(Ph)Br$ is also possible (Scheme 3, B) as both of these isomers can react with phenylacetylene to produce *cis*-$Pd(PPh_3)_2(CCPh)Ph$ (Scheme 3, routes C and C′, respectively). The formation of the *trans*-$Pd(PPh_3)_2(CCPh)Ph$ complex is possible from *cis*-

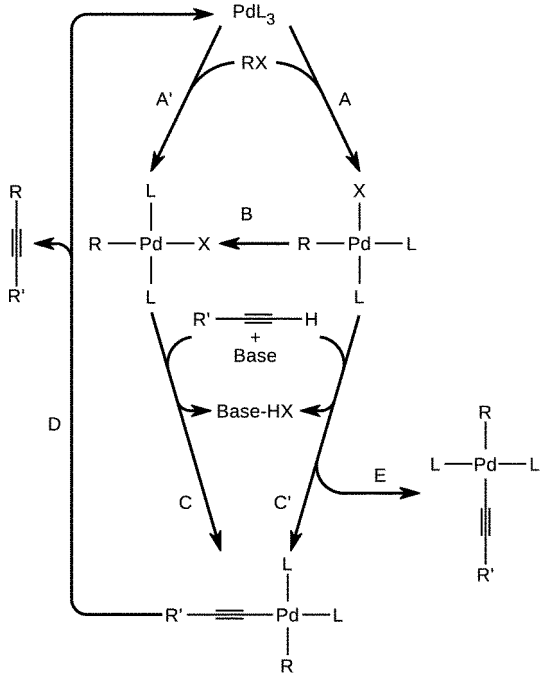

Scheme 3. Mechanism of the copper-free Sonogashira cross-coupling reaction.

$Pd(PPh_3)_2(Ph)Br$ (Scheme 3, E). The last step of the catalytic cycle is reductive elimination (Scheme 3, D), where diphenylacetylene is formed and the catalyst is regenerated.

CONCLUSIONS

The mechanism of the copper-free Sonogashira cross-coupling reaction is a complicated system of reaction pathways. The energetically most favoured reaction mechanism is composed of four steps: oxidative addition, *cis–trans* isomerization, deprotonation, and reductive elimination (A, B, C, and D in Scheme 3). On the other hand, the oxidative addition, which leads directly to the *trans*-product, and the deprotonation step starting from the *cis*-$Pd(PPh_3)_2(Ph)Br$ complex (A′ and C′, respectively, in Scheme 3) are energetically close to the lowest energy pathway. These pathways can be described as "shortcuts in the reaction", as they reduce the number of reaction steps in the catalytic cycle to three and all these reaction pathways can be of importance in experimental conditions.

ACKNOWLEDGEMENTS

The authors thank the Estonian Academy of Sciences and the Hungarian Academy of Sciences for the Estonian–Hungarian Joint Research Project 2007–2009. This work was supported by the Estonian Science Foundation (grants Nos 7199 and 8809), Estonian Ministry of Education and Research Targeted Financing project No. SF0180120s08, and Graduate School on Functional Materials and Technologies, EU Social Funds project 1.2.0401.09-0079.

REFERENCES

1. Dieck, H. A. and Heck, F. R. Palladium catalyzed synthesis of aryl, heterocyclic and vinylic acetylene derivatives. *J. Organomet. Chem.*, 1975, **93**, 259–263.
2. Cassar, L. Synthesis of aryl- and vinyl-substituted acetylene derivatives by the use of nickel and palladium complexes. *J. Organomet. Chem.*, 1975, **93**, 253–257.
3. Sonogashira, K., Tohda, Y., and Hagihara, N. A convenient synthesis of acetylenes: catalytic substitutions of acetylenic hydrogen with bromoalkenes, iodoarenes and bromopyridines. *Tetrahedron Lett.*, 1975, **16**, 4467–4470.
4. Chinchilla, R. and Nájera, C. The Sonogashira reaction: a booming methodology in synthetic organic chemistry. *Chem. Rev.*, 2007, **107**, 874–922.
5. Komáromi, A., Tolnai, G. L., and Novák, Z. Copper-free Sonogashira coupling in amine–water solvent mixtures. *Tetrahedron Lett.*, 2008, **49**, 7294–7298.
6. Chen, L.-P., Hong, S.-G., and Hou, H.-Q. Theoretical study on the mechanism of Sonogashira coupling reaction. *Chin. J. Struct. Chem.*, 2008, **27**, 1404–1411.
7. Fairlamb, I. J. S., O'Brien, C. T., Lin, Z., and Lam, K. C. Regioselectivity in the Sonogashira coupling of 4,6-dichloro-2-pyrone. *Org. Biomol. Chem.*, 2006, **4**, 1213–1216.
8. Chen, L.-P. and Chen, H.-P. DFT investigation on the mechanism of Pd(0) catalyzed Sonogashira coupling reaction. *Chin. J. Struct. Chem.*, 2011, **30**, 1289–1297.
9. Sikk, L., Tammiku-Taul, J., and Burk, P. Computational study of copper-free Sonogashira cross-coupling reaction. *Organometallics*, 2011, **30**, 5656–5664.
10. Sikk, L., Tammiku-Taul, J., Burk, P., and Kotschy, A. Computational study of the Sonogashira cross-coupling reaction in the gas phase and in dichloromethane solution. *J. Mol. Mod.*, 2012, **18**, 3025–3033.
11. García-Melchor, M., Pacheco, M. C., Nájera, C., Lledos, A., and Ujaque, G. Mechanistic exploration of the Pd-catalyzed copper-free Sonogashira reaction *ACS Catal.*, 2012, **2**, 135–144.
12. Amatore, C. and Pfluger, F. Mechanism of oxidative addition of palladium(0) with aromatic iodides in toluene, monitored at ultramicroelectrodes. *Organometallics*, 1990, **9**, 2276–2282.
13. Besora, M., Gourlaouen, C., Yates, B., and Maseras, F. Phosphine and solvent effects on oxidative addition of CH_3Br to $Pd(PR_3)$ and $Pd(PR_3)_2$ complexes. *Dalton Trans.*, 2011, **42**, 11089–11094.
14. Sun, W.-J., Chu, W., Yu, L.-J., and Jiang, C.-F. Ligand size effect on PdL_n oxidative addition with aryl bromide: a DFT study. *Chin. J. Chem. Phys.*, 2010, **23**, 175–179.
15. Mitchell, E. A., Jessop, P. G., and Baird, M. C. A kinetics study of the oxidative addition of bromobenzene to $Pd(PCy_3)_2$ (Cy = cyclohexyl) in a nonpolar medium: the influence on rates of added PCy_3 and bromide ion. *Organometallics*, 2009, **28**, 6732–6738.
16. Kozuch, S., Amatore, C., Jutand, A., and Shaik, S. What makes for a good catalytic cycle? A theoretical study of the role of an anionic palladium(0) complex in the cross-coupling of an aryl halide with an anionic nucleophile. *Organometallics*, 2005, **24**, 2319–2330.
17. Gooßen, L. J., Koley, D., Hermann, H., and Thiel, W. The mechanism of the oxidative addition of aryl halides to Pd-catalysts: a DFT investigation. *Chem. Commun.*, 2004, **19**, 2141–2143.
18. Amatore, C., Jutand, A, Lemaitre, F., Lucricard, J., Kozuch, S., and Shaik, S. Formation of anionic palladium(0) complexes ligated by the trifluoroacetate ion and their reactivity in oxidative addition. *J. Organomet. Chem.*, 2004, **689**, 3728–3734.
19. Amatore, C., Azzabi, M., and Jutand, A. Role and effects of halide ions on the rates and mechanisms of oxidative addition of iodobenzene to low-ligated zerovalent palladium complexes $Pd^0(PPh_3)_2$. *J. Am. Chem. Soc.*, 1991, **113**, 8375–8384.
20. Barrios-Landeros, F., Carrow, B. P., and Hartwig, J. F. Autocatalytic oxidative addition of PhBr to $Pd(P^tBu_3)_2$ via $Pd(P^tBu_3)_2(H)(Br)$. *J. Am. Chem. Soc.*, 2008, **130**, 5842–5843.
21. Casado, A. L. and Espinet, P. On the configuration resulting from oxidative addition of RX to $Pd(PPh_3)_4$ and

the mechanism of the *cis*-to-*trans* isomerization of [PdRX(PPh_3)$_2$] complexes (R = aryl, X = halide). *Organometallics*, 1998, **17**, 954–959.
22. Goossen, L. J., Koley, D., Hermann, H. L., and Thiel, W. Mechanistic pathways for oxidative addition of aryl halides to palladium(0) complexes: a DFT study. *Organometallics*, 2005, **24**, 2398–2410.
23. Soheili, A., Albaneze-Walker, J., Murry, J. A., Dormer, P. G., and Hughes, D. L. Efficient and general protocol for the copper-free Sonogashira coupling of aryl bromides at room temperature. *Org. Lett.*, 2003, **5**, 4191–4194.
24. Amatore, C., Jutand, A., and Suarez, A. Intimate mechanism of oxidative addition to zerovalent palladium complexes in the presence of halide ions and its relevance to the mechanism of palladium-catalyzed nucleophilic substitutions. *J. Am. Chem. Soc.*, 1993, **115**, 9531–9541.
25. Chinchilla, R. and Nájera, C. Recent advances in Sonogashira reactions. *Chem. Soc. Rev.*, 2011, **40**, 5084–5121.
26. Ljungdahl, T., Bennur, T., Dallas, A., Emtenäs, H., and Mårtensson, J. Two competing mechanisms for the copper-free Sonogashira cross-coupling reaction. *Organometallics*, 2008, **27**, 2490–2498.
27. Frisch, M. J., Trucks, G. W., Schlegel, H. B., Scuseria, G. E., Robb, M. A., Cheeseman, J. R. et al. *Gaussian 09*. Gaussian, Inc., Wallingford, CT, 2009.
28. Becke, A. D. Density-functional thermochemistry. V. Systematic optimization of exchange–correlation functionals. *J. Chem. Phys.*, 1997, **107**, 8554–8560.
29. Grimme, S. Semiempirical GGA-type density functional constructed with a long-range dispersion correction. *J. Comput. Chem.*, 2006, **27**, 1787–1799.
30. Dunning, T. H. Gaussian basis sets for use in correlated molecular calculations. I. The atoms boron through neon and hydrogen. *J. Chem. Phys.*, 1989, **90**, 1007–1023.
31. Schuchardt, K. L., Didier, B. T., Elsethagen, T., Sun, L., Gurumoorthi, V., Chase, J., Li, J., and Windus, T. L. Basis set exchange: a community database for computational sciences. *J. Chem. Inf. Model.*, 2007, **47**, 1045–1052.
32. Feller, D. The role of databases in support of computational chemistry calculations. *J. Comp. Chem.*, 1996, **17**, 1571–1586.
33. Ardura, D., López, R., and Sordo, T. L. Relative Gibbs energies in solution through continuum models: effect of the loss of translational degrees of freedom in bimolecular reactions on Gibbs energy barriers. *J. Phys. Chem. B*, 2005, **109**, 23618–23623.
34. Gonzalez, C. and Schlegel, H. B. An improved algorithm for reaction path following. *J. Chem. Phys.*, 1989, **90**, 2154–2161.
35. Gonzalez, C. and Schlegel, H. B. Improved algorithms for reaction path following: higher-order implicit algorithms. *J. Chem. Phys.*, 1991, **95**, 5853–5860.
36. Marenich, A. V., Cramer, C. J., and Truhlar, D. G. Universal solvation model based on solute electron density and on a continuum model of the solvent defined by the bulk dielectric constant and atomic surface tensions. *J. Phys. Chem. B*, 2009, **113**, 6378–6396.
37. Cramer, C. J. *Essentials of Computational Chemistry: Theories and Models*. Wiley, 2003.
38. Fitton, P. and Rick, E. A. The addition of aryl halides to tetrakis (triphenylphosphine) palladium(0). *J. Organomet. Chem.*, 1971, **28**, 287–291.
39. Rau, S., Lamm, K., Görls, H., Schöffel, J., and Walther, D. Bi- and trinuclear oxalamidinate complexes of palladium as catalysts in the copper-free Sonogashira reaction and in the Negishi reaction. *J. Organomet. Chem.*, 2004, **689**, 3582–3592.
40. García-Melchor, M., Fuentes, B., Lledós, A., Casares, J. A., Ujaque, G., and Espinet, P. Cationic intermediates in the Pd-catalyzed Negishi coupling. Kinetic and density functional theory study of alternative transmetalation pathways in the Me–Me coupling of $ZnMe_2$ and *trans*-[PdMeCl($PMePh_2$)$_2$]. *J. Am. Chem. Soc.*, 2011, **133**, 13519–13526.

Vasevaba Sonogashira ristkondensatsioonireaktsiooni modelleerimine: otseteed reaktsioonimehhanismis

Lauri Sikk, Jaana Tammiku-Taul ja Peeter Burk

Orgaanilises sünteesis on laialdast rakendust leidnud ristkondensatsioonireaktsioonid, mille alla kuuluvad mitmed siirdemetallide katalüüsitud süsinik-süsiniksideme tekkereaktsioonid. Sonogashira reaktsiooni puhul kasutatakse katalüsaatorina pallaadiumiühendit ja kaaskatalüsaatorina vaskhalogeniidi. Sel viisil sünteesitakse arüülhalogeniidide ja atsetüleeni derivaatide vahelisel reaktsioonil diasendatud atsetüleeni derivaate. Samas võib vase juuresolek põhjustada atsetüleeni derivaatide vahelist kondensatsiooni, mistõttu on välja arendatud mitmed vasevaba Sonogashira kondensatsioonireaktsiooni tüübid.

Traditsiooniline Sonogashira reaktsioon on mitmeetapiline, koosnedes oksüdatiivsest liitumisest, *cis*-*trans*-isomerisatsioonist, ümbermetallimisest ja redutseerivast elimineerimisest. Antud töös uuriti *sec*-butüülammooniumbromiidi katalüüsitud fenüülbromiidi oksüdatiivset liitumist Pd(PPh_3)$_3$ katalüsaatorile ja *trans*-Pd(PPh_3)$_2$(Ph)Br kompleksi reaktsiooni fenüülatsetüleeniga. Arvutusteks kasutati tihedusfunktsionaaliteooria B97D/cc-pVDZ meetodit ja SMD solvatatsiooni mudelit. Erinevalt traditsioonilisest oksüdatiivse liitumise mehhanismist on ammooniumsoola juuresolekul katalüüsitud reaktsiooni korral saaduseks *trans*-Pd(PPh_3)$_2$(Ph)Br ja isomerisatsioonietapp jääb

vahele. Teise ülesandena uuriti ümbermetallimist, mis võib alata ka *cis*-$Pd(PPh_3)_2(Ph)Br$ kompleksist. See on eelkõige oluline bidentaatsete ligandide korral, kus *trans*-$Pd(PPh_3)_2(Ph)Br$ kompleksi moodustumine ei ole võimalik. Neid kaht reaktsiooniteed võib käsitleda kui otseteid vasevaba Sonogashira kondensatsioonireaktsiooni mehhanismis, kuna etappide arv katalüütilises tsüklis väheneb kolmeni.